

Journal of

[www. biophotonics-journal.org](http://www.biophotonics-journal.org)

BIOPHOTONICS

 WILEY-VCH

REPRINT

FULL ARTICLE

Multi-dimensional fluorescence microscopy of living cells

Herbert Schneckenburger^{*,1,2}, Michael Wagner¹, Petra Weber¹, Thomas Bruns¹, Verena Richter¹, Wolfgang S. L. Strauss², and Rainer Wittig²

¹ Hochschule Aalen, Institut für Angewandte Forschung, Beethovenstr. 1, 73430 Aalen, Germany

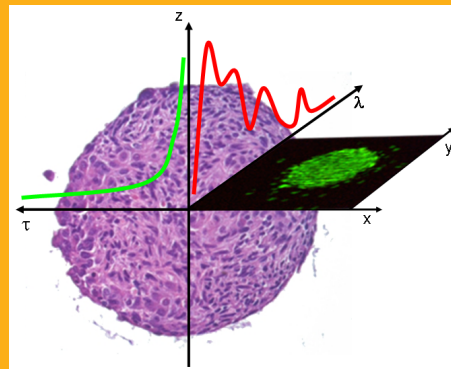
² Institut für Lasertechnologien in der Medizin und Meßtechnik an der Universität Ulm, Helmholtzstr. 12, 89081 Ulm, Germany

Received 9 September 2010, revised 19 October 2010, accepted 5 November 2010

Published online 22 November 2010

Key words: fluorescence microscopy, living cells, NADH, structured illumination, TIRFM, spectral imaging, FLIM, light dose

An overview on fluorescence microscopy with high spatial, spectral and temporal resolution is given. In addition to 3D microscopy based on confocal, structured or single plane illumination, spectral imaging and fluorescence lifetime imaging microscopy (FLIM) are used to probe the interaction of a fluorescent molecule with its micro-environment. Variable-angle total internal reflection fluorescence microscopy (TIRFM) permits selective measurements of cell membranes or cell-substrate topology in the nanometre scale and is also combined with spectral or time-resolved detection. In addition to single cells or cell monolayers, 3-dimensional cell cultures are of increasing importance, since they are more similar to tissue morphology and function. All methods reported are adapted to low dose of illumination, which is regarded as a key parameter to maintain cell viability. Applications include cancer diagnosis and cell tomography under different physiological conditions.



Multi-dimensional microscopy with spatial (3D), spectral and temporal resolution.

1. Introduction

Spatial resolution is a key parameter in optical microscopy. While light diffraction commonly limits lateral as well as axial resolution, further restrictions are due to a low focal depth at high magnification, i.e. images from a focal plane are often superposed by out-of-focus light. To overcome this problem, laser scanning techniques have been developed, where

information from a focal plane is selected either by a pinhole (confocal microscopy [1]) or by multiphoton excitation of distinct object planes [2, 3]. Laser scanning microscopy (LSM), however, is a rather complex technique, which often needs high light exposure and long measuring times. Therefore, axial resolution has also been introduced in (conventional) wide field microscopy using structured illumination [4]. By imaging an optical grid in various

* Corresponding author: e-mail: herbert.schneckenburger@htw-aalen.de, Tel.: +49 7361 5763401

(commonly three) positions of a sample and application of an appropriate algorithm, an image from the focal plane can be resolved, whereas out-of-focus light is eliminated. More recent techniques use a 3-dimensional interference pattern, permitting doubling of optical resolution in lateral as well as in axial direction [5]. Structured illumination, however, needs numerous light exposures for imaging various planes of a 3-dimensional sample, so that total light dose and measuring times may be similar to LSM. Only a few techniques with lower light exposure have been reported, so far. Those techniques include single plane illumination microscopy (SPIM) or light sheet fluorescence microscopy (LSFM), where only those planes of a sample are irradiated which are examined simultaneously [6], as well as total internal reflection fluorescence microscopy (TIRFM) [7, 8], where the surface of a sample (e.g. cell membrane) is illuminated selectively, such that damage to the whole cell is limited.

As reported recently, light dose plays a predominant role in fluorescence microscopy of living cells, since power densities of microscope illumination often exceed that of solar irradiance (100 mW/cm^2 or $1 \text{ nW}/\mu\text{m}^2$) by several orders of magnitude. While living cells tolerate a total light dose between about 10 J/cm^2 and 200 J/cm^2 corresponding to a time of 100 s up to 2,000 s of solar irradiation [9], considerably higher light doses are often attained by highly focusing optics in fluorescence microscopy. Light dose should, therefore, be one of the main criteria for selection of an appropriate method of live cell microscopy. A further prerequisite is that microscopes must be adapted to biological samples of different geometry, e.g. tissue samples or 3-dimensional cell cultures, which are more similar to tissue morphology and function than conventional 2-dimensional cell cultures on microscope slides [10].

In multi-dimensional microscopy spatial resolution is often combined with high spectral or temporal resolution, thus resulting in spectral imaging [11, 12] or fluorescence lifetime imaging microscopy (FLIM) [13, 14]. In addition to precise localization of fluorescent probes these techniques often permit to measure intermolecular interactions with their micro-environment. Non-radiative (Förster resonance) energy transfer (FRET) from a donor to an acceptor molecule [15] plays an important role in this context, since intermolecular distances below 10 nm can be detected reliably. Finally, polarization microscopy has proven to be a helpful tool, e.g. for measuring molecular rotations and for probing cellular viscosity or membrane fluidity [12, 14].

It is the main purpose of the present paper to show some valuable methods of multidimensional microscopy and to discuss their applicability to living cells. In this context novel designs, strict limitation of

the applied light dose and avoidance of extrinsic fluorescent markers play an increasing role.

2. Materials and methods

2.1 Cell systems

Experiments described in this paper were carried out with human glioblastoma cells either U373-MG cells obtained from the European Collection of Cell Cultures (ECACC No. 89081403) or genetically engineered U251-MG cells kindly supplied by Prof. Jan Mollenhauer, Dept. of Molecular Oncology, University of South Denmark, Odense. In one subclone of those U251 cells the tumour suppressor gene PTEN was over-expressed and activated, such that these cells exhibit a reduced tumorigenic potential and may be regarded as less malignant. Another subclone was generated by transfection with a plasmid encoding for a redox-sensitive green fluorescent protein (Grx1-roGFP2, kindly supplied by Dr. Tobias P. Dick, German Cancer Research Centre, Heidelberg) [16]. Cells were cultivated either as monolayers on glass slides as described elsewhere [9] or as spheroids of about $300 \mu\text{m}$ in diameter. These spheroids were grown within individual cavities of a microtiter plate coated with agarose gels. After addition of a cellular suspension, cell adhesion was prevented, and growth of spheroids was favoured.

2.2 3D Microscopy

Commonly, lateral resolution in fluorescence microscopy is defined by the Abbé criterion $\Delta x = 0.61\lambda/A_{\text{Obj}}$ with λ corresponding to the wavelength of light and A_{Obj} to the numerical aperture of the objective lens, while axial resolution can be defined by the depth of focus $\Delta z = n\lambda/A_{\text{Obj}}^2$. With high aperture objective lenses ($A_{\text{Obj}} = 1.45$) minimum values $\Delta x \approx 200 \text{ nm}$ and $\Delta z \approx 350 \text{ nm}$ are thus attained. In laser scanning microscopy (LSM) the pinhole size can be adjusted such that information is recovered only from the focal depth Δz , and full 3D information is obtained from a series of images recorded with multiple steps of Δz .

Structured illumination can be performed by imaging an optical grid into the plane of the sample at 3 different phase angles. An algorithm described in Ref. [4] permits to calculate an (unstructured) image I from the focal plane, whereas out-of-focus contributions are eliminated. Axial resolution again depends on the numerical aperture of the objective lens as well as on the spatial frequency of the grid and may

attain values below 1 μm . In 3-dimensional spheroids, however, selection of individual cell layers with $\Delta z \approx 10 \mu\text{m}$ may be more important than sub-cellular resolution. Therefore, a modular system has been developed, where an optical grid is imaged on a glass slide (containing the sample) with an objective lens of moderate magnification (5–20 \times) and numerical aperture (0.15–0.50). Exchangeable light emitting diodes (LEDs) are used for illumination, and an integrating high resolution CCD camera (e.g. ProgRes C10, Jenoptik GmbH, Jena, Germany) for image detection.

While axial resolution of LSM and structured illumination microscopy can be easily varied in the micrometer and sub-micrometer range, total internal reflection fluorescence microscopy (TIRFM) is limited to the nanometre scale. In TIRFM incident light is totally reflected on a cell-substrate interface with a variable penetration depth d of the evanescent electromagnetic field depending on the angle θ of incidence. When a fluorescent dye is distributed rather homogeneously either in the cytoplasm or in the plasma membrane, and when fluorescence intensity I_F is determined as a function of θ , cell-substrate distances can be calculated with nanometre precision, as described in Ref. [17]. Two custom-made illumination devices have recently been reported. While in a first one the angle of incidence of a parallel laser beam can be varied in multiple steps with a precision of $\pm 0.25^\circ$ [17], this angle is fixed at $67.5 \pm 1.3^\circ$ in a second one permitting a penetration depth $d = 110 \pm 35 \text{ nm}$ [20]. This latter condenser unit contains a focusing lens for selective illumination of small fluorescent samples, e.g. single cells.

2.3 Spectral and fluorescence lifetime imaging

Microspectral imaging combines spatial and spectral resolution in microscopy by insertion of dispersive elements, e.g. gratings or interference filters (for a review see [11]). Depending on the individual technique, spectral images are recorded simultaneously, sequentially or in a scanning mode, and specific algorithms are used for calculation of biophysical parameters. In the present setup a set of broad band interference filters is used in combination with an upright fluorescence microscope (Axioplan 1, Carl Zeiss Jena, Germany).

In fluorescence lifetime imaging microscopy (FLIM) the fluorescence decay time is measured for each pixel of a microscopic image. This can be done by time-correlated single photon counting in laser scanning microscopy (LSM) experiments, where for each fluorescence photon the time delay after the

preceding laser pulse is registered, as described in Ref. [23]. Another possibility is to use fast camera technology and to detect the fluorescence intensity within two time gates shifted by an interval Δt between one another. In this case a fluorescence lifetime $\tau = \Delta t / \ln(I_A/I_B)$ can be calculated from the intensities I_A and I_B measured within the two time gates. Only in the case of mono-exponential decays τ corresponds to the real fluorescence lifetime; otherwise it has to be regarded as an effective lifetime containing information of all fluorescent components. In the present setup samples are excited by picosecond pulses of a laser diode (LDH 375 or LDH 400 with driver PDL 800-B, PicoQuant, Berlin, Germany; wavelengths: 375 nm or 391 nm; pulse energy: 12 pJ, pulse duration: 55 ps, repetition rate: 40 MHz), and time-gated fluorescence images are recorded by an image intensifying camera system (Picostar HR 12 image intensifier coupled to a cooled CCD camera; LaVision, Göttingen, Germany) with a time resolution of 200 ps. Generally time gates with a gate width of 1 ns and different delay time with respect to the preceding laser pulse are used for fluorescence lifetime imaging.

3. Results

The potential of 3D microscopy with structured illumination is shown in Figure 1 for a 3-dimensional cell spheroid containing a redox-sensitive green fluorescent protein. Its architecture is illustrated in an histological section after hematoxylin-eosin staining (A). Upon conventional wide field microscopy almost no substructure can be deduced (B), whereas upon structured illumination individual cells from a layer of $\Delta z \approx 10 \mu\text{m}$ become clearly visible (C) and may be further analyzed. Due to the compact optical setup a light dose of only 0.04 J/cm is necessary to record 3 images needed for reconstruction of a cell monolayer, and even multiple exposure appears well tolerable for living cells.

To achieve axial resolution in single cell experiments, structured illumination or laser scanning microscopy with high aperture objective lenses are methods of choice. For selective measurements of cell surfaces, e.g. plasma membranes, variable-angle TIRFM provides increasing resolution down to the range of a few nanometers. This has recently been demonstrated for fluorescent markers of the cytoplasm or cell membranes, when cell-substrate topology has been evaluated upon depletion of cholesterol or after photodynamic therapy [18]. In addition, TIRFM experiments permitted to study protein-protein interactions with high precision, e.g. in the pathogenesis of Alzheimer's disease [19] or in sensing of apoptosis [20].

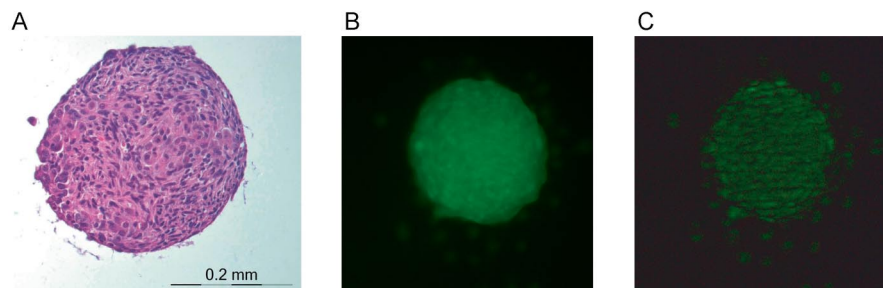


Figure 1 (online color at: www.biophotonics-journal.org) 3-dimensional spheroid of U251-MG glioblastoma cells containing the redox-sensitive green fluorescent protein Grx1-roGFP2; (A) histological section after hematoxylin-eosin staining; (B) conventional fluorescence image; (C) sectional view from the focal plane ($\Delta z \approx 10 \mu\text{m}$); excitation wavelength: 470 nm; fluorescence detection: $\geq 515 \text{ nm}$, image size: $450 \times 450 \mu\text{m}$.

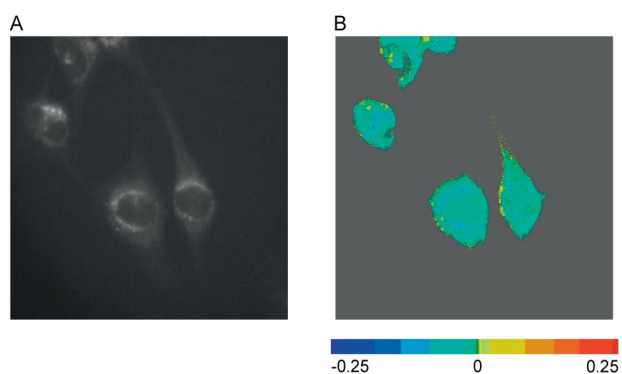


Figure 2 (online color at: www.biophotonics-journal.org) Intrinsic fluorescence of U251-MG glioblastoma cells detected at $\lambda \geq 415 \text{ nm}$ (A) and protein binding parameter $\text{PBP} = (I_{450} - I_{490}) / (I_{450} + I_{490})$ including scale (B); excitation wavelength: 375 nm; image size: $140 \times 140 \mu\text{m}$.

Spectral imaging and fluorescence lifetime imaging (FLIM) have previously been applied to various topics on membrane dynamics and intermolecular interactions [12, 19, 20, 24]. While those experiments have been performed with fluorescent dyes or fluorescent proteins, intrinsic fluorophores with overlapping emission spectra and comparably low quantum yields are subject of present investigation. In Figure 2 intrinsic fluorescence of U251-MG glioblastoma cells is depicted, which upon excitation at $\lambda = 375 \text{ nm}$ is dominated by broad spectral bands with maxima around 440–450 nm and 470–490 nm. Those bands have been attributed to protein-bound and free coenzyme nicotinamide adenine dinucleotide (NADH) [21, 22]. When fluorescence is measured in different spectral ranges, e.g. at $450 \pm 20 \text{ nm}$ (I_{450}) and $490 \pm 20 \text{ nm}$ (I_{490}), a protein binding parameter $\text{PBP} = (I_{450} - I_{490}) / (I_{450} + I_{490})$

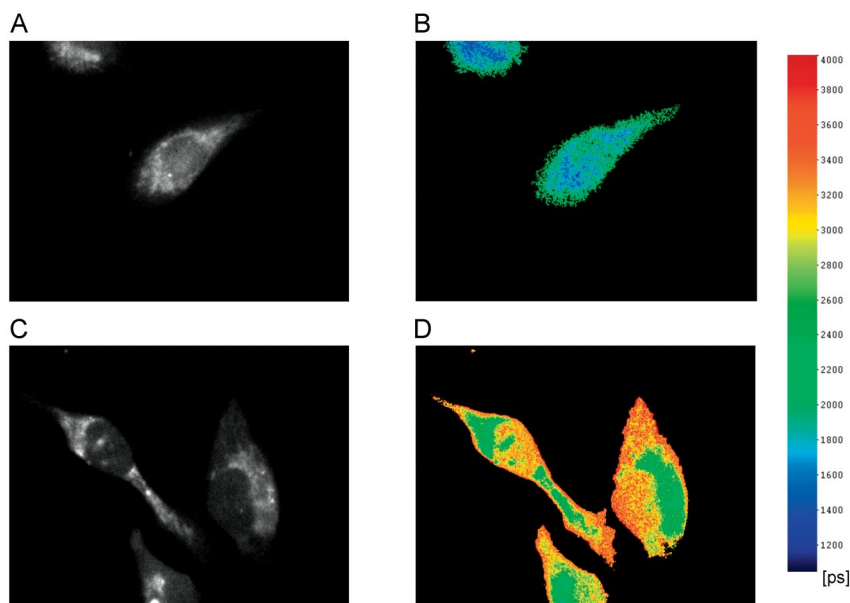


Figure 3 (online color at: www.biophotonics-journal.org) Intensities (A, C) and effective lifetimes (B, D) of intrinsic fluorescence of U251-MG glioblastoma cells (A, B) and U251-MG cells with an activated PTEN suppressor gene (C, D); excitation wavelength: 375 nm; fluorescence detection: $\geq 415 \text{ nm}$; image size: $140 \times 110 \mu\text{m}$.

can be calculated, as depicted in Figure 2. While U251-MG glioblastoma cells are characterized by diffuse as well as by granular fluorescence around the cell nucleus (A), the lowest PBP values are observed within the granules (B). This may be helpful to identify fluorescent organelles and to distinguish cells of different malignancy. FLIM may support those experiments, as demonstrated in Figure 3. While fluorescence patterns of U-251-MG control cells (A) and cells with an activated tumor suppressor gene (C) are similar, the effective fluorescence lifetimes of the tumor cells (B) are lower than those of the less malignant cells (D). This may be due to different contributions of free and protein-bound NADH with fluorescence lifetimes of about 0.5 ns and 2.5–3.0 ns, respectively.

4. Discussion

Microscopic methods with diffraction limited resolution have been described above. Only in variable-angle TIRFM an axial resolution below 10 nm, and thus beyond the so-called Abbé criterion was attained. Further methods of super-resolution microscopy are presently developed by several groups. Some promising approaches, e.g. stochastic optical resolution microscopy (STORM) [25, 26] or photo-activated localization microscopy (PALM) [27], are based on single molecule detection, where each molecule is measured n times, such that local precision is improved by a factor $n^{-1/2}$ and reaches values of 10–20 nm. Single molecule experiments, however, need power densities around $100 \text{ nW}/\mu\text{m}^2$, which is 100–1000 times higher than solar irradiance ($1 \text{ kW}/\text{m}^2$ corresponding to $1 \text{ nW}/\mu\text{m}^2$), so that cells are expected to survive no longer than a few seconds. Another method of super-resolution microscopy is stimulated emission depletion microscopy (STED) [28] permitting a lateral resolution of about 30 nm at an average power density of $30 \mu\text{W}/\mu\text{m}^2$ (calculated for a 300 mW laser which scans a surface of $100 \times 100 \mu\text{m}$). This is 30,000 times more than solar irradiance and does not appear appropriate for measurements of living cells.

In conventional LSM and wide field microscopy the power density of illumination can often be limited to about $1 \text{ nW}/\mu\text{m}^2$ which corresponds to solar irradiance and appears to be appropriate for life cell experiments up to a few minutes (depending on the wavelength of illumination and additional application of exogenous fluorophores [9]). The limit of viability, however, may be exceeded upon multiple exposures, e.g. when a larger number of cell layers is examined. This problem may be overcome by single plane illumination microscopy (SPIM) [6], where only those layers of a sample

Table 1 Irradiance and maximum time of illumination for maintaining viability (according to [9]) of U373-MG glioblastoma cells at a wavelength $\lambda = 514 \text{ nm}$ (* = average value applied in laser scanning microscopy; ** = estimated value).

Method	Irradiance [$\text{nW}/\mu\text{m}^2$]	Max. time of illumination [s]
LSM	1 (*)	1,000
structured illumination	1	1,000
SPIM	≤ 1	10,000 (**)
TIRFM	1	3,000
single molecule methods	100–1,000	1–10
STED	30,000 (*)	not relevant

are exposed to light, which are recorded simultaneously. Therefore, SPIM appears to be the method of choice for measurements of numerous layers (e.g. of 3-dimensional cell cultures) or for experiments of long exposure time. Also TIRFM appears to be a favourable method for maintaining cell viability, since the evanescent electromagnetic field penetrates only a small distance into the cell, thus reducing cellular damage, as previously demonstrated [9]. An overview on relevant irradiances and estimated times of illumination for maintaining cell viability is given in Table 1 for different methods of 3D microscopy.

A combination of microscopic methods with high axial, spectral and temporal resolution seems to be appropriate for solving numerous questions in cell biology and in vitro diagnostics. In each case, the appropriate technique of spectral or fluorescence lifetime imaging should be considered carefully. For example, a FLIM technique based on time-correlated single photon counting provides an optimum of information, whereas fast camera technology permits shorter measuring times and lower light exposure. Of particular interest are FRET and related techniques permitting to probe intermolecular distances in the nanometre range. Also techniques without fluorescence staining and based e.g. on intrinsic fluorescence or Raman scattering are of increasing interest in view of future in vivo applications.

Acknowledgments Present research is funded by Land Baden-Württemberg, Europäische Union Europäischer Fonds für die regionale Entwicklung, Baden-Württemberg-Stiftung gGmbH, and Bundesministerium für Bildung und Forschung (BMBF). Skilful technical assistance by C. Hintze is gratefully acknowledged.



Herbert Schneckenburger is a professor of Physics, Optics, and Biophotonics at Hochschule Aalen and private lecturer of the Medical Faculty of the University of Ulm. His research is concentrated on optical spectroscopy, microscopy and in-vitro diagnostics.



Michael Wagner received his Master degree in Photonics from Hochschule Aalen. He is preparing his Ph.D. thesis at the Medical Faculty of the University of Ulm and Hochschule Aalen. His research is concentrated on modern techniques of microscopy and membrane dynamics of cancer cells.



Petra Weber received her diploma of Nutrition Science from the University of Hohenheim and is presently preparing her Ph.D. thesis at the Medical Faculty of the University of Ulm and Hochschule Aalen.



Thomas Bruns received his Master degree in Photonics from Hochschule Aalen and is presently preparing his Ph.D. thesis at the University of Ulm and Hochschule Aalen. He is working as a scientist in the fields of biophotonics, microscopy and in-vitro diagnostics.



Verena Richter is a graduate engineer (FH) in Optoelectronics/Laser technology and is currently preparing her Master thesis in Photonics at Hochschule Aalen.

Wolfgang Strauss studied chemistry at the University of Ulm and is a senior scientist at the ILM in Ulm. His research focuses on photodynamic therapy and fluorescence diagnostics of cancer as well as on cell model systems for various fluorescence microscopic techniques.



Rainer Wittig is a molecular biologist and group leader at the ILM in Ulm. His research focuses on cancer and photobiology, three-dimensional cell cultures, and laser-based cell manipulation.

References

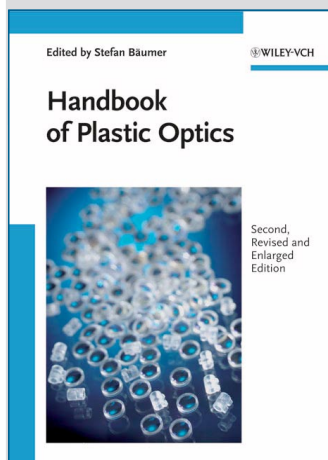
- [1] J. Pawley, Handbook of Biological Confocal Microscopy (Plenum Press, New York, NY, USA, 1990).
- [2] W. Denk, J. H. Strickler, and W. W. Webb, *Science* **248**, 73–76 (1990).
- [3] K. König, *J. Microsc.* **200**, 83–86 (2000).
- [4] M. A. A. Neil, R. Juskaitis, and T. Wilson, *Opt. Lett.* **22**, 1905–1907 (1997).
- [5] M. G. L. Gustafsson, L. Shao, P. M. Carlton, C. J. R. Wang, I. N. Golubovskaya, W. Z. Cande, D. A. Agard, and J. W. Sedat, *Biophys. J.* **94**, 4957–4970 (2008).
- [6] J. Huisken, J. Swoger, F. del Bene, J. Wittbrodt, and E. H. K. Stelzer, *Science* **305**, 1007–1009 (2004).
- [7] D. Axelrod, *J. Cell Biol.* **89**, 141–145 (1981).
- [8] H. Schneckenburger, *Curr. Opin. Biotechnol.* **16**, 13–18 (2005).
- [9] M. Wagner, P. Weber, T. Bruns, W. S. L. Strauss, R. Wittig, and H. Schneckenburger, *Int. J. Mol. Sci.* **11**, 956–966 (2010).

- [10] L. A. Kunz-Schughart, J. P. Freyer, F. Hofstaedter, and R. Ebner, *J. Biomol. Screen.* **9**, 273–285 (2004).
- [11] Y. Garini, Y. I. T. Young, and G. McNamara, *Cytometry* **69A**, 735–747 (2006).
- [12] P. Weber, M. Wagner, and H. Schneckenburger, *J. Biomed. Opt.* **15**, 046017/1–046017/5 (2010).
- [13] E. B. van Munster and T. W. Gadella, *Adv. Biochem. Eng. Biotechnol.* **95**, 43–75 (2005).
- [14] J. A. Levitt, D. R. Matthews, S. M. Ameer-Beg, and K. Suhling, *Curr. Opin. Biotechnol.* **20**, 28–36 (2009).
- [15] T. Förster, *Ann. Physik* **2**, 55–75 (1948).
- [16] M. Gutscher, A. L. Pauleau, L. Marty, T. Brach, G. H. Wabnitz, Y. Samstag, A. J. Meyer, and T. P. Dick, *Nat. Methods* **5**, 553–559 (2008).
- [17] K. Stock, R. Sailer, W. S. L. Strauss, M. Lyttek, R. Steiner, and H. Schneckenburger, *J. Microsc.* **211**, 19–29 (2003).
- [18] M. Wagner, P. Weber, W. S. L. Strauss, H.-P. Lassalle, and H. Schneckenburger, *Adv. Opt. Technol.* **2008**, 254317:1–254317:7 (2008).
- [19] C. A. F. von Arnim, B. von Einem, P. Weber, M. Wagner, D. Schwanzar, R. Spoelgen, W. S. L. Strauss, and H. Schneckenburger, *Biochem. Biophys. Res. Commun.* **370**, 207–212 (2008).
- [20] B. Angres, H. Steuer, P. Weber, M. Wagner, and H. Schneckenburger, *Cytometry* **75A**, 420–427 (2009).
- [21] T. Galeotti, G. D. V. vanRossum, D. H. Mayer, and B. Chance, *Eur. J. Biochem.* **17**, 485–496 (1970).
- [22] J.-M. Salmon, E. Kohen, P. Viallet, J. G. Hirschberg, A. W. Wouters, C. Kohen, and B. Thorell, *Photochem. Photobiol.* **36**, 585–593 (1982).
- [23] W. Becker, *Advanced time-correlated single photon counting techniques* (Springer, Berlin – Heidelberg – New York, 2005).
- [24] H. Schneckenburger, K. Stock, M. Lyttek, W. S. L. Strauss, and R. Sailer, *Photochem. Photobiol. Sci.* **3**, 127–131 (2004).
- [25] E. Betzig, G. H. Patterson, R. Sougrat, O. W. Lindwasser, S. Olenych, J. S. Bonifacino, M.W. Davidson, J. Lippincott-Schwartz, and H. F. Hess, *Science* **313**, 1642–1645 (2006).
- [26] M. J. Rust, M. Bates, and X. Zhuang, *Nat. Meth.* **3**, 793–796 (2006).
- [27] S. T. Hess, T. P. K. Girirajan, and M. D. Mason, *Biophys. J.* **91**, 4258–4272 (2006).
- [28] K. I. Willig, B. Harke, R. Medda, and S. W. Hell, *Nat. Meth.* **4**, 915–918 (2007).

Edited by STEFAN BÄUMER
Philipps Eindhoven

Handbook of Plastic Optics

2nd revised and enlarged edition



2010. XII, 296 pages,
approx. 80 figures, 60 in color.
Hardcover.
€ 109.- / £ 90.- / US\$ 175.-
ISBN: 978-3-527-40940-2

A coherent overview of the current status of injection molded optics, describing in detail all aspects of plastic optics, from design issues to production technology and quality control.

This updated second edition is supplemented by a chapter on the equipment and process of injection wells as well as a look at recent applications.

The contributors, each one a leading expert in their discipline, have either a background in or strong ties to the industry, thus combining a large amount of practical experience.

With its focus firmly set on practical applications, this is an indispensable reference for all those working in optics research and development.

WILEY-VCH • P.O. Box 10 11 61 • 69451 Weinheim, Germany
Fax: +49 (0) 62 01 - 60 61 84
e-mail: service@wiley-vch.de • http://www.wiley-vch.de

Register now for the free
WILEY-VCH Newsletter!
www.wiley-vch.de/home/pas

 **WILEY-VCH**